

Synthesis and Electrochemical Properties of Oligo- and Poly(thienylphenylamine)s

Kimihisa Yamamoto, Masayoshi Higuchi, Kumiko Uchida, and Yojiro Kojima

Macromolecules, **2002**, 35 (15), 5782-5788 • DOI: 10.1021/ma011018c

Downloaded from <http://pubs.acs.org> on February 9, 2009

More About This Article

Additional resources and features associated with this article are available within the HTML version:

- Supporting Information
- Links to the 3 articles that cite this article, as of the time of this article download
- Access to high resolution figures
- Links to articles and content related to this article
- Copyright permission to reproduce figures and/or text from this article

[View the Full Text HTML](#)



Synthesis and Electrochemical Properties of Oligo- and Poly(thienylphenylamine)s

Kimihisa Yamamoto,* Masayoshi Higuchi, Kumiko Uchida, and Yojiro Kojima

Department of Chemistry, Faculty of Science & Technology, Keio University, Yokohama, 223-8522 Japan

Received June 12, 2001; Revised Manuscript Received April 19, 2002

ABSTRACT: The oxidative polymerization of tris(thienylphenyl)amine derivatives was performed in acetonitrile by electrochemical and chemical methods. Oligomers were synthesized by stepwise coupling using coupling reactions. The polymer prepared using the trifunctional monomer on a Pt electrode showed significantly better redox behavior compared to that of the linear polymeric analogue. The branching polymers exhibit conductivity of 2–6 S/cm, which is more than 1 order of magnitude greater than the analogous linear polymer. The electropolymerization of trifunctional monomers provides the formation of a large amount of redox active polymers with a large capacity (ca. 40 mC/cm²) and a good redox activity in the electron transfer of ferrocene on the electrode.

Introduction

Conjugated molecules such as polythiophene or triphenylamine are expected to be good hole transporting materials in thin-layered solar batteries¹ or in electroluminescent devices.² However, these monomeric molecules^{3–5} are not sufficient to exhibit high hole transport efficiency because of their crystallinity, are difficult to mold, and/or have a low thermal stability. Recently, polymers with a dendritic and/or hyperbranched structure have received more attention as amorphous and soluble polymers. The dendritic structure also provides interesting functions,^{6–8} e.g., energy transfer, a photochemical antenna, and stepwise metal-assembling. Not only are the amorphous properties very interesting, but also the electronic and redox ones for the branched polymers.^{9,10} The carrier transport is an important factor contributing to the electronic conductivity of the electronically conductive materials. The three-dimensional structure of branched polymers might allow improved carrier transport to provide quite different electrical properties. It is of interest to determine whether the electronic properties of the dendritic polymers are better than those of the analogous linear polymers.

In this study, we focused on triphenylamine containing redox molecules¹¹ and synthesized tris[4-(2-thienyl)phenyl]amine (PT1N), 4,4',4''-tris[4-(2-bithienyl)phenyl]amine (PT2N), and 4,4',4''-tris[4-(2-terthienyl)phenyl]amine (PT3N) as trifunctional monomers for the dendritic polymers. Two synthetic methods were employed for the polymer preparation. The novel poly(thienylphenylamine)s were obtained by chemical oxidative polymerization and by electropolymerization in acetonitrile. The electrochemical properties such as redox activity, electrocatalytic activity, and conductivity are compared between the branched polymers and the corresponding linear polymers.

Experimental Section

Chemicals. All reagent grade chemicals were purchased from Aldrich, Tokyo Kasei Co., Ltd., and Kantoh Kagaku Co., Inc., and were used without further purification. The supporting electrolytes were recrystallized before use.

Spectroscopic Measurements. The UV–vis spectra were obtained using a Shimadzu UV-2400PC spectrometer with a

ITO (indium–tin oxide) electrode. The infrared spectrum was obtained on a potassium bromide pellet using a Shimadzu FT-IR 8300 spectrometer. The MALDI–TOF mass spectra were measured by a Shimadzu-Kratos COMPACT MALDI SEQ using dithranol as the matrix. The FAB mass spectra were measured by a Shimadzu mass spectrometer using benzyl alcohol as the matrix.

Electrochemical Measurements. The electrochemical measurements were carried out in a conventional two-compartment cell. The solutions were kept under an atmosphere of dry N₂. A Pt disk electrode was used as the working electrode and was polished before each experiment with a 0.05 μm alumina paste. The auxiliary electrode, a coiled platinum wire, was separated from the working solution by a fine-porosity frit. The reference electrode was a commercial Ag/Ag⁺ one, which was placed in the main cell compartment. The formal potential of the ferrocene/ferrocenium couple was 0.076 V vs this reference electrode in acetonitrile. All potentials are quoted with respect to this Ag/Ag⁺ reference electrode. A BAS Co., Ltd., model 660 electrochemical workstation was employed. Tetrabutylammonium tetrafluoroborate (TBABF₄, 0.2 M) was used as the supporting electrolyte. The formal potential was normalized to the ferrocene/ferrocenium couple in acetonitrile. Cyclic voltammetry was carried out at a scanning rate of 100 mV/s. The rotating disk voltammograms were recorded using the same apparatus at the same electrode rotated at 2000 rpm and scanned at 10 mV/s. Differential pulse voltammograms of the oligomers were measured in dichloromethane–TBABF₄ solution. The pulse width and the scanning width were 90 mV, and the range was from 0 to 1.3 V.

Determination of Electron-Transfer Rate. The electron-transfer rates between ferrocene and the resulting polymers were determined by chronocoulometry in acetonitrile solution on the polymer-modified electrode in the presence of 10 mM ferrocene. The measurement was carried out in the same apparatus using the same instruments as for the cyclic voltammetry. The initial applied potential was –0.2 V, and the potential was stepped to 0.4 V with a pulse width of 0.9 s.

Measurement of Conductivity. The polymer films were prepared on a Pt hyperbranched microelectrode (length 2 mm, width 10 μm, space 5 μm). The conductivity of the resulting polymers was measured by cyclic voltammetry swept between 0 and 0.7 V in acetonitrile–TBABF₄(0.2 M) electrolyte, where the counter electrode was applied at 0.2 V constant potential as the drain voltage.

Synthesis of PT1N Oligomers. (a) Preparation of Mono- or Di-Br-Substituted PT1N. A solution of 1-bromo-succinimide (NBS) (362 mg, 2.0 mmol) in CH₂Cl₂ (60 mL) was

added dropwise to a solution of PT1N (1.0 g, 2.0 mmol) in CH_2Cl_2 (40 mL) and AcOH (20 mL). The reaction solution was stirred at room temperature for 1 h. Saturated aqueous NaHCO_3 solution was added, and the product was extracted with CH_2Cl_2 . The organic layer was washed with brine, dried (Na_2SO_4), and evaporated. Purification of the residue by column chromatography (silica gel; hexane- CH_2Cl_2 7:1) furnished unchanged PT1N (271 mg; 21%), 1BrPT1N (508 mg; 44%), and 2BrPT1N (272 mg; 27%). 1BrPT1N: ^1H NMR (400 MHz, CDCl_3) δ 6.96 (d, $J = 4.0$ Hz, 1H), 6.99 (d, $J = 4.0$ Hz, 1H), 7.05 (dd, $J = 3.6, 5.2$ Hz, 2H), 7.10 (d, $J = 8.8$ Hz, 2H), 7.11 (d, $J = 8.8$ Hz, 4H), 7.23 (dd, $J = 3.6, 5.2$ Hz, 4H), 7.39 (d, $J = 8.8$ Hz, 2H), 7.51 (d, $J = 8.8$ Hz, 4H). ^{13}C NMR (100 MHz, CDCl_3) δ 110.6, 122.5, 122.6, 124.1, 124.3, 124.6, 126.6, 127.0, 128.1, 128.3, 129.6, 130.9, 144.0, 145.7, 146.4, 147.0. FAB-MS [m/z] = 569 ($M + 2$). 2BrPT1N: ^1H NMR (400 MHz, CDCl_3) δ 6.96 (d, $J = 4.0$ Hz, 2H), 6.99 (d, $J = 4.0$ Hz, 2H), 7.05 (dd, $J = 3.6, 5.2$ Hz, 1H), 7.10 (d, $J = 8.8$ Hz, 4H), 7.11 (d, $J = 8.8$ Hz, 2H), 7.23 (dd, $J = 3.6, 5.2$ Hz, 4H), 7.39 (d, $J = 8.8$ Hz, 4H), 7.51 (d, $J = 8.8$ Hz, 2H). ^{13}C NMR (100 MHz, CDCl_3) δ 110.7, 122.5, 122.6, 124.3, 124.4, 124.8, 126.6, 127.0, 128.1, 128.5, 129.8, 130.9, 144.0, 145.6, 146.2, 146.8. FAB-MS [m/z] = 647 ($M + 2$).

(b) Preparation of the Mono-Stannyl-Substituted PT1N Bis(thienylphenyl)(4-trimethylstannylthienylphenyl)amine. To a THF solution (25 mL) of PT1N (502 mg, 1.02 mmol) was added *n*-butyllithium (1.3 mL, 2.04 mmol) dropwise at -78°C . The mixture was stirred at room temperature for 5 min. Tri-*n*-butyltin chloride (0.55 mL, 2.04 mmol) was added dropwise at -78°C , and the mixture was stirred at room temperature for 5 min. Water was added, and the product was extracted with EtOAc. The organic layer was washed with brine, dried (Na_2SO_4), and evaporated. Purification of the residue by column chromatography (silica gel treatment with 10% Et_3N -hexane; hexane) furnished 1-Sn(*n*-Bu) $_3$ PT1N (320 mg; 40%). ^1H NMR (270 MHz, CDCl_3) δ 0.91 (t, $J = 7.3$ Hz, 9H), 1.12 (m, 6H), 1.36 (m, 6H), 1.58 (m, 6H), 7.06 (d, $J = 3.8$ Hz, 2H), 7.11 (d, $J = 8.4$ Hz, 6H), 7.12 (d, $J = 3.6$ Hz, 1H), 7.23 (d, $J = 3.8$ Hz, 4H), 7.36 (d, $J = 3.6$ Hz, 1H), 7.49 (d, $J = 8.4$ Hz, 4H), 7.52 (d, $J = 8.4$ Hz, 2H).

Dimer. Under N_2 , 1SnPT1N (104 mg, 0.13 mmol) in THF (10 mL) was added dropwise to the mixture of 1BrPT1N (75.9 mg, 0.13 mmol) and $\text{Pd}(\text{PPh}_3)_4$ (7.7 mg, 6.65 μmol). The reaction mixture was refluxed for 1 h and cooled at room temperature. The reaction solution was diluted with THF, and the product was purified by column chromatography (silica gel; hexane-THF 8:1) furnished dimer (115 mg; 88%). ^1H NMR (400 MHz, $\text{C}_4\text{D}_8\text{O}$) δ 7.04 (dd, $J = 3.9, 5.4$ Hz, 4H), 7.14 (d, $J = 8.8$ Hz, 12H), 7.22 (d, $J = 3.9$ Hz, 2H), 7.31 (d, 10H), 7.57 (d, $J = 8.8$ Hz, 12H). ^{13}C NMR (100 MHz, $\text{C}_4\text{D}_8\text{O}$) δ 123.4, 124.2, 125.1, 125.3, 125.4, 127.2, 127.6, 127.7, 128.0, 128.8, 129.5, 136.2, 142.7, 144.0, 146.5, 146.7. MALDI-TOF MS = 980.

Trimer and Tetramer. (a) Trimer: Following the above procedure for the dimer using 2BrPT1N (30 mg, 0.46 μmol), 1SnPT1N (175 mg, 224 μmol), and $\text{Pd}(\text{PPh}_3)_4$ (5.3 mg, 4.62 μmol) in THF (40 mL), the trimer was obtained. Purification by column chromatography (silica gel; hexane-THF 6:1) produced the trimer (24 mg; 35%). ^1H NMR (400 MHz, CD_2Cl_2) δ 7.08 (dd, $J = 3.6, 5.2$ Hz, 5H), 7.15 (d, $J = 8.8$ Hz, 18H), 7.18 (dd, $J = 3.6$ Hz, 4H), 7.21 (d, $J = 3.6$ Hz, 4H), 7.27 (d, $J = 5.2$ Hz, 5H), 7.29 (d, $J = 3.6$ Hz, 5H), 7.55 (d, $J = 8.8$ Hz, 18H). ^{13}C NMR (100 MHz, $\text{C}_4\text{D}_8\text{O}$) δ 123.4, 124.2, 125.0, 125.1, 125.3, 125.5, 127.3, 127.7, 128.7, 130.0, 130.7, 131.2, 137.1, 137.9, 143.7, 145.0, 147.6, 147.9. MALDI-TOF MS = 1470.

(b) Tetramer: 3BrPT1N (25.3 mg, 32 μmol), 1SnPT1N (150 mg, 192 μmol), and $\text{Pd}(\text{PPh}_3)_4$ (5.0 mg, 4.23 μmol) in THF (67 mL) were used and purification by column chromatography (silica gel; hexane-THF 4:1) produced the tetramer (6.0 mg; 10%). ^1H NMR (400 MHz, CD_2Cl_2) δ 7.08 (dd, $J = 3.5, 5.1$ Hz, 6H), 7.15 (d, $J = 8.8$ Hz, 24H), 7.18 (d, $J = 3.6$ Hz, 6H), 7.21 (d, $J = 3.6$ Hz, 4H), 7.22 (d, $J = 3.6$ Hz, 2H), 7.27 (d, $J = 5.1$ Hz, 6H), 7.28 (d, $J = 3.5$ Hz, 6H), 7.55 (d, $J = 8.8$ Hz, 24H). ^{13}C NMR (Hz, $\text{C}_4\text{D}_8\text{O}$) δ 123.4, 124.3, 125.1, 125.5, 127.3, 127.6,

127.7, 128.7, 130.0, 130.2, 130.7, 137.1, 137.2, 143.7, 143.8, 145.0, 147.6, 147.9. MALDI-TOF MS = 1959.

Synthesis of Polymers. (a) Chemical Oxidative Polymerization. The branched polymers, pPT1Nc, pPT2Nc, and pPT3Nc, were obtained in 97–98% yield by chemical oxidative polymerization of PT1N, PT2N, and PT3N with ferric chloride as the oxidant in CH_2Cl_2 . FeCl_3 (389 mg, 2.4 mmol) was added to the PT1N solution (5 mL of CH_2Cl_2). The reaction solution was stirred for 4 h at room temperature under N_2 . The reaction solution was then precipitated into MeOH (500 mL) and filtered. The solid was reduced from the oxidizing form by a 1 N NH_3 methanol solution and filtered. This procedure was repeated five times. The polymer, pPT1Nc, was obtained in 97% yield (401 mg). The same procedures were employed for the polymerization of PT2N and PT3N. The concentrations of PT2N and PT3N in the reaction mixture were 16.9 and 6.25 mM, respectively, because of solubility limitations. pPT2Nc and pPT3Nc were each obtained in 98% yield.

(b) Electropolymerization of Tris(thienylphenylamine)s. The electropolymerization of the monomers (1 mM) was carried out by cyclic potential sweeps in the range from 0 to 1.1 V vs Ag/Ag^+ on a Pt disk electrode ($\phi = 2$ mm) using same apparatus and instruments as that for cyclic voltammetry. The supporting electrolyte was tetrabutylammonium tetrafluoroborate (0.2 M). The solvent was a mixture of acetonitrile and dichloromethane [v/v: 10/1 (PT1N), 1/1 (PT2N), and 1/10 (PT3N)].

Results and Discussion

Synthesis of Monomers^{12–19} and Oligomers. As precursors to the branched polymers, the tris[4-(2-oligothienyl)phenyl]amines (PT1N, PT2N, and PT3N) with a thienyl, bithienyl, or terthienyl group were synthesized (Scheme 1). The synthesis of PT1N was carried out through the cross-coupling reaction of the MgBr-substituted thiophene with tris(bromophenyl)amine using a Pd catalyst. PT1N was isolated in 79% yield. PT1N was successfully brominated at the 4-position of the thienyl group with NBS. A similar procedure for PT1N was used to synthesize PT2N. Brominated PT1N reacts with the Grignard thiophene to yield PT2N in 76%. Terthiophene boronic acid for the Suzuki coupling reaction was prepared by the reaction of lithium terthiophene with triethyl borate in the presence of 1 N HCl. The Suzuki coupling with tris-(bromophenyl)amine using a Pd catalyst produced PT3N in 32% yield. PT3N has poor solubility compared to that of the starting materials, such as tris(bromophenyl)amine and terthienylboronic acid. During the reaction PT3N is precipitated in MeCN. PT3N can then be isolated by filtration. These monomers were characterized by NMR and IR spectra, mass spectrometry, and elemental analysis.

As monomers of the analogous linear polymers, which were used for a comparison with the branched polymers, bis(thienylphenyl)(4-methylthienylphenyl)amine (MePT1N) and bis(thienylphenyl)(4-bromophenyl)amine (Br-PT1N) were also synthesized through cross-coupling using a Pd catalyst. BrPT1N was also synthesized using the same procedure as for PT1N. The cross-coupling of the MgBr-substituted methylthiophene with BrPT1N produced MePT1N.

As model compounds, the dimer, trimer, and tetramer of PT1N were prepared in order to investigate their electrochemical properties and spectra. The oligomers of PT1N were synthesized through cross-coupling of the Br-substituted PT1N and the stannyl-substituted one using a Pd catalyst. As raw materials for the dimer and trimer, the mono- and dibromo-substituted PT1N derivatives were prepared in one pot by bromination in

Scheme 1

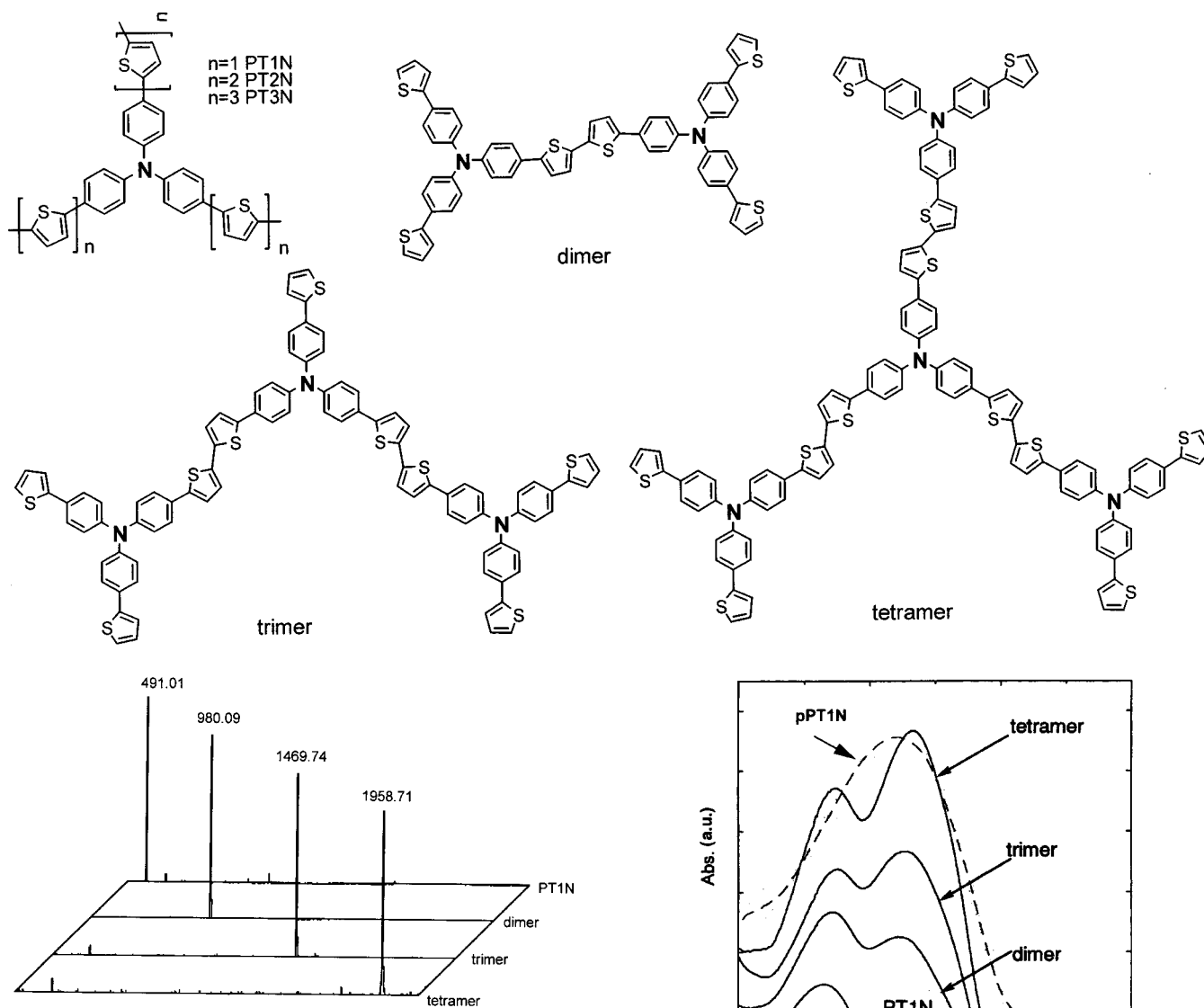


Figure 1. TOF mass spectra of oligomers.

the presence of an equimolar molar amount of NBS. The mono- and dibromo-substituted PT1Ns were isolated in 44 and 27% yield, respectively. The monosubstituted PT1N was prepared with *n*-BuLi and (*n*-Bu)₃SnCl from the dibromo compound. The coupling was confirmed by the ¹³C NMR spectrum of the dimer, which shows the quaternary carbon coupled thiophene at 137 ppm. The mass fragment peak agrees with the molecular weight of the oligomers (Figure 1).

Physicochemical Properties of Oligomers. The UV-vis spectra of the oligomers show two characteristic absorption bands in THF (Figure 2). For the dimer, the peak at 372 nm is attributed to the terminal thiophene ring because the absorption band almost agrees with that of PT1N at 366 nm. The absorption band at 426 nm is attributed to the π - π^* transition of the bithiophene moiety. The absorption band of the thiophene ring at the linking unit shifts to a longer wavelength because of the extended π -conjugation. The absorption at ca. 430 nm increases as the absorption at ca. 370 nm decreases, which is emphasized by the increasing degree of oligomerization from the dimer to tetramer. The ratio of the absorption at ca. 430 nm to that at ca. 370 nm was determined by a peak separation method using Gauss-

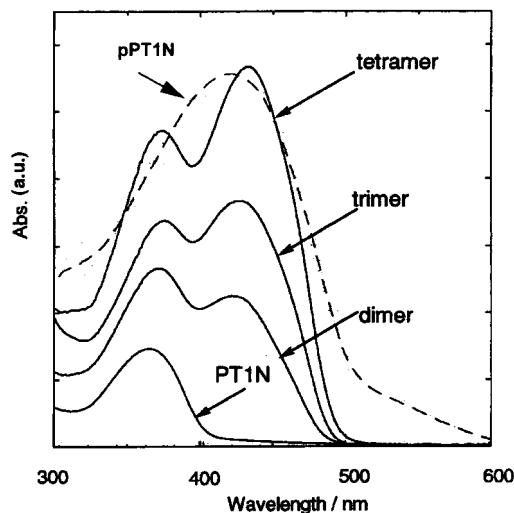
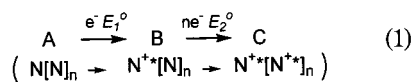
Figure 2. UV-vis spectra of PT1N and oligomers (6.0×10^{-6} M) in THF and pPT1N film (dotted line) prepared on ITO electrode; the absorbance was normalized.

Table 1. UV-vis Absorption of PT1N Oligomers in Dichloromethane

oligomer	end unit (nm)	binding unit (nm)	absorption ratio end/binding
monomer	366		
dimer	372	426	1.3
trimer	376	428	1.1
tetramer	374	438	0.9

ian curve fitting. The ratio decreases with the increasing degree of oligomerization (Table 1).

The oligomers can undergo multistep electron-transfer reactions of the type (oligomers{N[N]_n}; *n* = 1 dimer, *n* = 2 trimer, *n* = 3 tetramer; the symbol "+*" means cation radical). It is well-known that the electrostatic repulsion results in broadening of the differential pulse voltammetry (DPV) wave (SI Figure 9 in Supporting Information).^{21,22} E_1^0 and E_2^0 of the oligomers in each



step could not be determined by DPV because the redox waves overlapped. The large interaction results in more splitting or broadening of the DPV oxidation waves compared to that of the monomer. DPV revealed broadening of the DPV wave with the increasing degree of oligomerization (Figure 3, Table 2). The tetramer shows the largest peak width of the DPV wave in the oligomers. These results support the idea that the cation radical of the tetramer is more stable than that of the trimer, and the cation radical may possibly exist not at the end group but at the branching moiety of the branched polymer.

The second peak in the DPV corresponds to the oxidation of the bithiophene units. The tetramer shows the lowest oxidation potential in the oligomers. The small potential gap ($\Delta E_{\text{am-thio}}$) between the amine site and the thiophene moiety means that electron- or hole-hopping is promoted by the thiophene moiety (Table 2).

Oxidative Polymerization. The polymers were obtained in more than 95% yield by chemical oxidative polymerization with FeCl_3 . The molecular weight of the hot α -chloronaphthalene-soluble portion of the resulting polymer was measured by high-temperature GPC analysis with a polystyrene standard. The weight-average molecular weights of pPT1Nc, pPT2Nc, and pPT3Nc were determined to be 6000, 18 000, and 13 200, respectively. The UV-vis spectrum of the THF-soluble portion in THF also shows the formation of the pPT1Nc oligomer. The electronic spectrum was similar to that of the tetramer. The ratio of the absorption at 430 nm to that at 370 nm was about 0.9.

Polymer films were obtained on the Pt electrode by sweeping the potential from 0 to 1.1 V vs Ag/Ag^+ in the monomer solution of acetonitrile-dichloromethane (Figure 1). Homogeneous pPT1Ne, pPT2Ne, and pPT3Ne films were formed on the electrode (see SI Figure 10).

The redox wave at 0.51 V is attributed to the radical cation formation of the amine moiety, and the oxidation at around 1.0 V is attributed to the formation of the cation radical of the thiophene group. The polymer growth at the electrode was confirmed by the increasing current in the cyclic voltammogram during electropolymerization by potential sweeping. The polymerization takes place at applied potentials above 1.0 V because the cation radical formed by the oxidation of the thiophene unit is the active species for the polymerization. The polymerization proceeds through the oxidative coupling of the thiophene rings.

Only a trace amount of the oligomer was extracted at room temperature with THF or α -chloronaphthalene from the polymer pPT1Ne film obtained by electropolymerization. This insolubility is caused by the formation of a high molecular weight polymer and high cross-linking because of the heterogeneous polymerization on the electrode surface, where high-concentration conditions of the oligomers are maintained. The thermal stabilities of the branched polymers, pPT1Ne, pPT2Ne, and pPT3Ne, were evaluated by thermogravimetric analysis under a N_2 atmosphere after reduction with NH_3 -methanol solution. The branched polymers show a high thermal stability above a $T_{d10\%}$ of 550 °C, the temperature of 10% weight loss. Thermogravimetric analysis of the branched polymers reveals a thermostability higher than common plastics. The high thermal

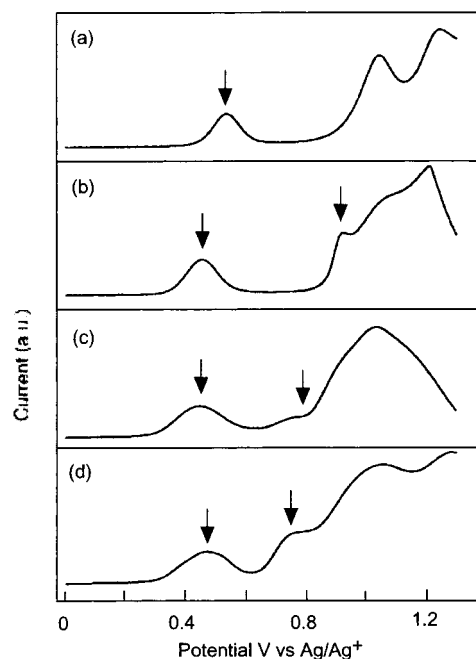


Figure 3. Differential pulse voltammetry (DPV) of oligomers (0.1 mM) in dichloromethane solution: (a) PT1N, (b) dimer, (c) trimer, (d) tetramer. Supporting electrolyte: TBABF₄ (0.1 M), pulse width 90 mV.

Table 2. Electrochemical Parameters of PT1N Oligomers in Dichloromethane

oligomer	$\Delta E_{1/2}^a$ (mV)	ΔE^b (mV)	E_{am}^c (V)	E_{thio}^d (V)	$\Delta E_{\text{am-thio}}^e$ (mV)
monomer			0.534		
dimer	130	52	0.922	0.456	466
trimer	164	81	0.800	0.460	340
tetramer	171	89	0.780	0.472	308

^a Half-width at half-maximum current of differential pulse voltammogram. ^b $\Delta E = E_1^0 - E_2^0$ in eq 1 was determined according to ref 20. ^c Redox potential of the bithiophene unit. ^d Redox potential of the amine site. ^e $E_{\text{am}}^c - E_{\text{thio}}^d$, reference electrode: Ag/Ag^+ .

stability is based on the cross-linking structure because the number of end groups in the branching polymer decreases by the cross-linking.

The polymer film, pPT1Ne, shows a broad peak at 420 nm without a detectable shoulder at 370 nm in the UV-vis spectrum, which is attributed to the end group (Figure 2). On the basis of the results of the oligomers, the small ratio of the absorption at ca. 430 nm to that at ca. 370 nm indicates a decrease in the end group due to the cross-linking.

The cross-linking formation is also supported by the IR results. The polymer film (pPT1Ne) shows a IR spectrum similar to the pPT1Nc polymer prepared by the oxidative polymerization with FeCl_3 . However, peak intensities around 700 cm^{-1} are different between pPT1Ne and pPT1Nc. The monomers and pPT1Ne show an absorption at 690 cm^{-1} , which is attributed to the C-H out-of-plane vibration of the neighboring 3 H at the end group of the thiophene ring (Figure 5). The quantity of the end group on the thiophene ring is estimated by the ratio of the IR peak intensity at 696 cm^{-1} vs 1599 cm^{-1} assigned to the vibration of the C=C bond on the phenylene ring because the ratio decreases in the following order (Table 3): monomer (PT1N) > 1-bromo-PT1N > 2-bromo-PT1N > 3-bromo-PT1N. The intensity of the THF-insoluble part of the

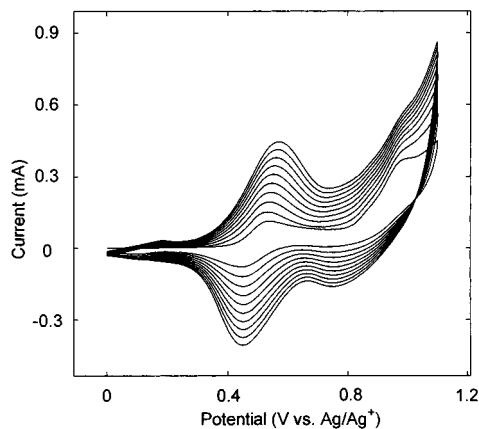


Figure 4. Cyclic voltammograms of PT1N (1 mM) during the electropolymerization on Pt disk electrode in acetonitrile. Electrolyte: TBABF₄ (0.2 M); scan rate: 100 mV/s.

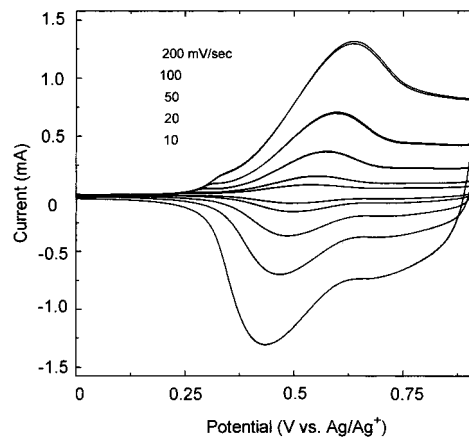


Figure 6. Cyclic voltammograms of pPT1Ne prepared by electropolymerization on Pt disk electrode in acetonitrile. Scan rate: 10, 20, 50, 100, and 200 mV/s.

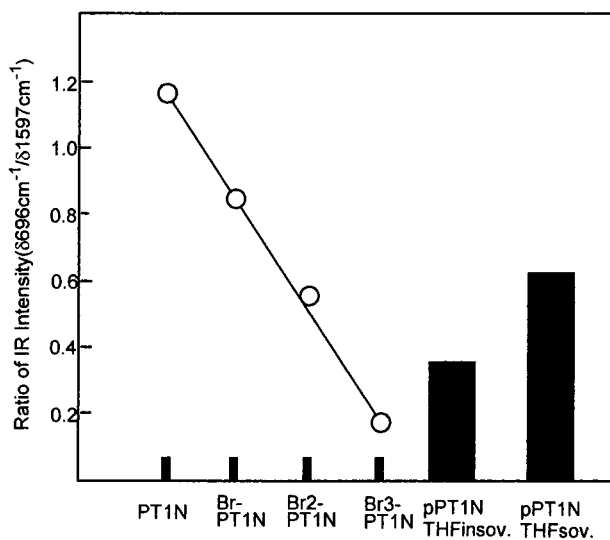


Figure 5. Ratio of IR band intensity of the end group in the pPT1Ne and tris(thienylphenylamine) derivatives.

Table 3. Electrochemical Properties of the Electrochemically Prepared Polymer Films in Acetonitrile

monomer	E° ^a (V) ^c	$E_{1/2}(\text{Fc})^b$ (V) ^c	rate constant k (10^3 cm s^{-1})	conductivity σ (S/cm^{-1})
PT1N	0.51	0.18	8.9	2.4
PT2N	0.53	0.14	9.1	4.1
PT3N	0.52	0.10	9.2	6.3
BrPT1N	0.52	0.26	7.7	0.081
MePT1N	0.56	0.30	8.6	0.61

^a Redox potential of the polymer films. ^b Half-wave potential in RDV of ferrocene on the polymer-modified electrode. ^c Ag/Ag⁺.

film is between that of 2-Br-PT1N and 3Br-PT1N. This indicates that cross-linking takes place during the electropolymerization.

Electrochemical Properties of Electrochemically Prepared Polymers. The redox properties of the resulting polymer films were confirmed by cyclic voltammetry. The resulting polymers show a redox wave at ca. 0.5 V vs Ag/Ag⁺ in acetonitrile-tetrabutylammonium tetrafluoroborate solution (Figure 6). The redox activity was not degraded even after 100 cyclic potential sweeps. The redox potentials attributed to the amine moiety were not drastically influenced by the length of the thiophene unit. The relationship between the scan

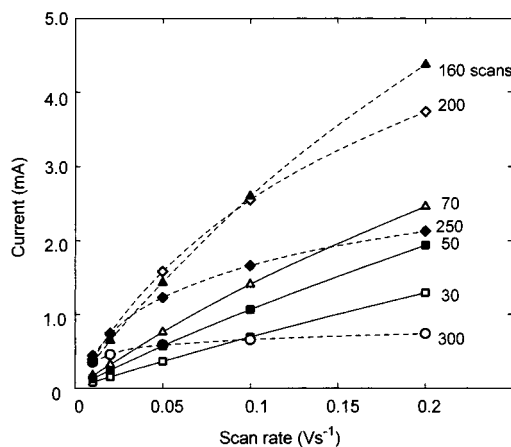


Figure 7. Redox activity of pPT1Ne polymers prepared by potential scanning (scan numbers in the figure). Relationship between the oxidation peak current and scan rate in the cyclic voltammetry on the polymer-modified electrode.

rate and the oxidation peak current of the polymer during the cyclic voltammetry is shown in Figure 7. In the thin-layered polymer, which is formed by the electropolymerization, the oxidation peak current is proportional to the scan rate, not its square, and the polymers possess good redox activity. These results indicate that the electrochemical process does not obey the diffusion process²² during the redox reaction of the polymer. By increasing the amount of the resulting polymer film, the linearity of the relation is collapsed due to reducing the redox activity. To quantitatively evaluate the redox responses of the polymers, the electric capacity and the oxidation peak current of the resulting polymers were sampled at the point with a 0.997 correlation coefficient in the plot v vs i . The electric capacity and the oxidation peak current of the branched polymers were superior to that of the corresponding linear polymers (Figure 8). Especially, the resulting branched polymer of PT2N showed the largest capacity (41.2 mC/cm^2) with good redox activity. PPT2N provides good redox activity on the electrode with capacity, that is, 4–5 times greater in comparison with those of the linear analogues.

These results indicate that the trifunctional monomers can form large amounts of corresponding polymers with good redox activity which can act as excellent conductive materials. Therefore, the increase in the redox current corresponding to the formation of the

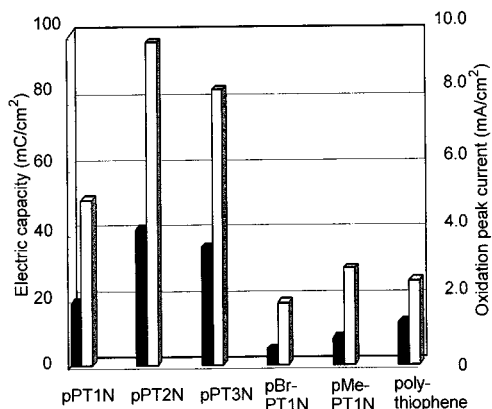


Figure 8. Redox activity of the polymers prepared by potential scanning. Electric capacity (black bar) in the redox reaction based on N/N^{+*} (potential sweep range: 0–0.8 V). Oxidation peak (white bar) in the redox reaction at 100 mV/s.

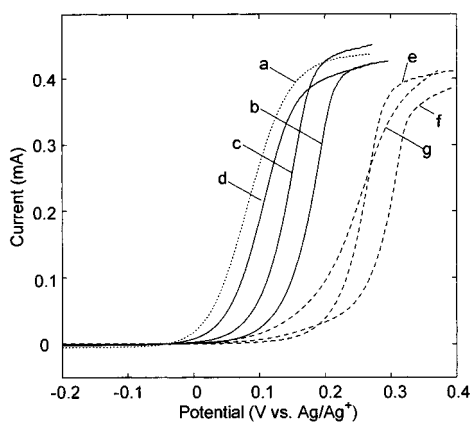


Figure 9. Rotating disk voltammograms of the oxidation of ferrocene on the polymer-modified Pt electrode in acetonitrile–0.2 M TBABF₄ solution: bare (a), pPT1Ne (b), pPT2Ne (c), pPT3Ne (d), pBrPT1Ne (e), pMePT1Ne (f), polythiophene (g). Scan rate: 10 mV/s; rotating rate: 2000 rpm.

polymer was observed during the cyclic voltammetry even after large scan numbers.

Electron transfer between the polymer and ferrocene was investigated in order to evaluate the redox response of the polymers.^{23,24} Rotating disk voltammetry of ferrocene was performed with the polymer modified electrode obtained by electropolymerization (Figure 9). The half-wave potential of the ferrocene/ferrocenium couple was observed at 0.18 V vs Ag/Ag⁺ on the pPT1N-modified electrode. Those of the pPT2N and pPT3N are located at 0.14 and 0.10 V vs Ag/Ag⁺, respectively. Oxidation of the ferrocene with electrodes covered with pPT1N, pPT2N, and pPT3N takes place at potentials lower than those of the analogous linear polymers, which shows the higher half-wave potential of about 200 mV. The resulting branched polymers efficiently mediated electron transfer from ferrocene to the Pt electrode. This result indicates that the branched polymers have a higher activity for the oxidation of ferrocene than the analogous linear polymers.

The electron-transfer rate constants between the resulting polymer film and ferrocene were estimated by chronocoulometry²⁵ in a ferrocene/acetonitrile solution to elucidate the redox activity. The rate constants of the electron transfer were determined to be around $(9.0 \pm 2) \times 10^{-3}$ cm/s. The electron transfer rate is not significantly affected by the structural difference between the branched and linear polymers.

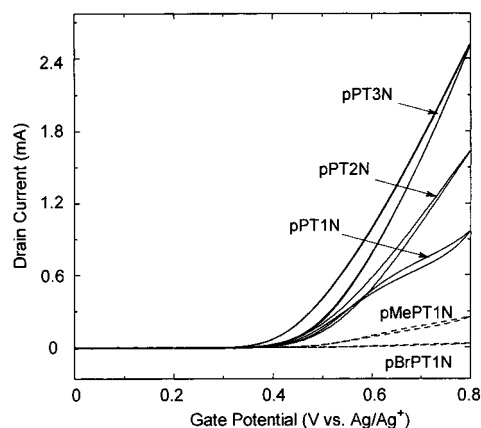


Figure 10. In situ conductivity measurement of the polymers in acetonitrile solution (supporting electrolyte: TBABF₄) on the interdigitated array electrode.

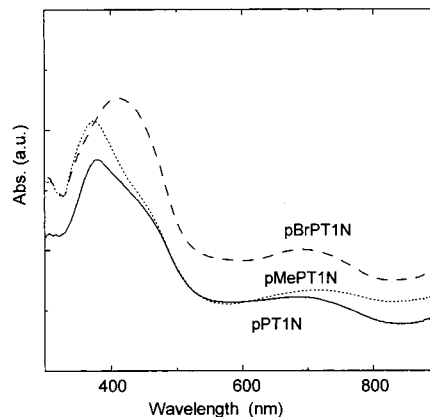


Figure 11. Spectro-electrochemistry of pPT1Ne, pBrPT1Ne, and pMePT1Ne in acetonitrile solution on a ITO electrode at 1.1 V.

The different redox activity behavior for ferrocene between the branched and the corresponding linear polymers is dominated by the conductivity of the resulting polymer. The conductivities of the polymers were measured using an interdigitated array electrode²⁶ modified with a polymer obtained by electropolymerization (Figure 10). The branched polymers of PT1N, PT2N, and PT3N show conductivities of 2.4, 4.1, and 6.3 S/cm, respectively. The analogous linear polymers of BrPT1N and MePT1N show conductivities of 0.081 and 0.61 S/cm, respectively. The conductivities of the branched polymers were more than 1 order of magnitude greater than those of the analogous linear ones. The higher conductivity of the branched polymers results in the oxidation of ferrocene at a lower potential.

The polymer films were generated on an ITO electrode by electropolymerization to perform spectro-electrochemical analysis. Using the polymer-modified ITO electrode, similar electronic absorption spectra attributed to the cation radical (Figure 11) were obtained. This means that the band gaps between the linear (MePT1N and BrPT1N) and branched polymer (pPT1Ne) are almost similar. These results support the fact that the numbers of carriers in the polymers are similar when compared with the linear one. The conduction mechanism is dominated by hole transfer. The intra- and intermolecular hopping mechanisms of the carriers are not different between the linear and branched polymers because these types of polymers are not conjugated. Therefore, the branched polymer maintains

multiple pathways for the carrier to provide the electronic conductivity even in the presence of defects in the polymer. The dendritic structure is advantageous for electron and hole transport. The higher conductivity results in the formation of a large amount of polymer with significantly better redox activity for the ferrocene.

Acknowledgment. This work was partially supported by a Grant-in-Aid for priority area (No. 13022263) and for Scientific Research (No. 12650870, 13555261, 13750821) from the Ministry of Education Science Foundation Culture, a Grant-in-Aid for Evaluative Technology (12407) from the Science and Technology Agency, and Kanagawa Academy Science and Technology Research Grant (Project No. 23).

Supporting Information Available: Description of the synthesis of monomers; IR spectra of pPT1Nc; UV-vis spectra of oligomers in THF; cyclic voltammograms of PT2N and PT3N, BrPT1N(a) and MePT1N(b), pPT2Ne(a) and pPT3Ne(b), and pBrPT1Ne(a) and pMEPT1Ne(b); redox activity of pPT2Ne and pPT3Ne; analysis for multielectron-transfer process; and AFM picture of pPT1Ne. This material is available free of charge via the Internet at <http://pubs.acs.org>.

References and Notes

- (1) Bach, U.; Lupo, D.; Comte, P.; Moser, J. E.; Weissortel, F.; Salbeck, J.; Spreitzer, H.; Gratzel, M. *Nature (London)* **1998**, *395*, 583.
- (2) Kuwabara, Y.; Ogawa, H.; Inada, H.; Noma, N.; Shirota, Y. *Adv. Mater.* **1994**, *6*, 677.
- (3) Shirota, Y.; Kobata, T.; Noma, N. *Chem. Lett.* **1989**, 1145.
- (4) Kunugi, Y.; Tabkovic, I.; Canavesi, A.; Miller, L. L. *Synth. Met.* **1997**, *89*, 227.
- (5) Tabkovic, I.; Kunugi, Y.; Canavesi, A.; Miller, L. L. *Acta Chem. Scand.* **1998**, *52*, 131.
- (6) Devadoss, C.; Bharathi, P.; Moore, J. S. *J. Am. Chem. Soc.* **1996**, *118*, 9635.
- (7) Pillow, J. N. G.; Halim, M.; Lupton, J. M.; Burn, P. L.; Samuel, I. D. W. *Macromolecules* **1999**, *32*, 5985.
- (8) (a) Jiang, D.-L.; Aida, T. *Nature (London)* **1997**, *388*, 454. (b) Yamamoto, K.; Higuchi, M.; Shiki, S.; Tsuruta, M.; Chiba, H. *Nature (London)* **2002**, *415*, 509.
- (9) Wienk, M. M.; Janssen, R. A. J. *J. Am. Chem. Soc.* **1997**, *119*, 4492.
- (10) Nishide, H. *Angew. Chem., Int. Ed. Engl.* **1998**, *37*, 2400.
- (11) Yamamoto, K.; Higuchi, M.; Uchida, K.; Kojima, Y. *Macromol. Chem. Rapid Commun.* **2001**, *22*, 266.
- (12) Muisck, K. Y.; Hu, Q. S.; Pu, L. *Macromolecules* **1992**, *25*, 1214.
- (13) Nakayama, J.; Konishi, T.; Murabayashi, S.; Hoshino, M. *Heterocycles* **1987**, *26*, 1793.
- (14) Kim, S. B.; Harada, K.; Yamamoto, T. *Macromolecules* **1998**, *31*, 988.
- (15) Miller, L. L.; Yu, Y. *J. Org. Chem.* **1995**, *60*, 6813.
- (16) Zhang, Q. T.; Tour, J. M. *J. Am. Chem. Soc.* **1997**, *119*, 5065.
- (17) Still, J. K. *Angew. Chem., Int. Ed. Engl.* **1986**, *25*, 508.
- (18) Sotzing, G. A.; Rwynolds, J. R.; Steel, P. J. *Chem. Mater.* **1996**, *8*, 882.
- (19) Bobacka, J.; Grzeszczuk, M.; Ivaska, A. *J. Electroanal. Chem.* **1997**, *427*, 63.
- (20) Richardson, D. E.; Taube, H. *Inorg. Chem.* **1981**, *20*, 1278.
- (21) Sutton, J. E.; Sutton, P. M.; Taube, H. *Inorg. Chem.* **1979**, *18*, 1017.
- (22) Kazarinov, V. E.; Levi, M. D.; Skundin, A. M.; Vorotyntsev, M. A. *J. Electroanal. Chem.* **1989**, *271*, 193.
- (23) Christie, J. H.; Lauer, G.; Osteryoung, R. A. *J. Electroanal. Chem.* **1964**, *7*, 60.
- (24) Zhu, S. S.; Swager, T. M. *J. Am. Chem. Soc.* **1997**, *119*, 12568.
- (25) Thackeray, J. W.; White, H. S.; Wrighton, M. S. *J. Phys. Chem.* **1985**, *89*, 5133.
- (26) Ofer, D.; Crooks, R. M.; Wrighton, M. S. *J. Am. Chem. Soc.* **1990**, *112*, 7869.

MA011018C